Analog ionospheric forecasts: Space weather forecasts by analogy with previous events

Leo F. McNamara,[1] Gregory J. Bishop,[1] and Judith A. Welsh[1]

Received 16 March 2010; revised 13 July 2010; accepted 20 October 2010; published 22 January 2011.

[1] Operational systems that take advantage of the ionosphere or for which the ionosphere is a major inconvenience require that deleterious changes to the ionosphere during geomagnetically disturbed intervals be forecast up to several days in advance, in order to allow mitigation procedures to be instituted. However, the reliability of current space weather models of the Sun, solar wind, magnetosphere and ionosphere is such that the consequential ionospheric forecasts depend too much on the uncertainties of the various models. It is no secret that the level of success of space weather forecasts is currently still a decade or two behind that achieved by the tropospheric weather forecasting community. As an interim solution to forecasting the low and midlatitude ionosphere, we propose the use of analog forecasts in which we look to the past to see what happened to the ionosphere during a historical interval for which the forecast geomagnetic conditions also applied. In order to investigate the concept of analog forecasts, we have analyzed Australian ionosonde values of NmF2 for ~200 disturbed intervals. While we do not expect analog forecasts to match the details of individual storms, we do expect them to provide users with the essential nature of a forecast ionospheric storm. The reliability of analog forecasts should increase as we gain experience and thus provide a standard of reliability that will eventually be reached by fully coupled space weather forecasts.

Citation: McNamara, L. F., G. J. Bishop, and J. A. Welsh (2011), Analog ionospheric forecasts: Space weather forecasts by analogy with previous events, *Radio Sci.*, *46*, RS1002, doi:10.1029/2010RS004399.

1. Introduction

[2] It should be pointed out that this is more of a concept paper than one that presents results of comparisons of a new model with observations. It does not apply to current capabilities so much as to what could be done in the future. We return to this point at the end of this section.

[3] The present study arose naturally out of the objectives of the AFRL Space Weather Forecasting Laboratory (SWFL) and the ongoing validation by AFRL of the global model of the ionosphere that is used by the Air Force Weather Agency (AFWA). SWFL is an AFRL project to evaluate existing space weather models, develop and validate new models, and make the best integrated suite of models available for use by AFWA and other government agencies.

[4] The model of the ionosphere used by AFWA is the Utah State University Global Assimilation of Ionospheric Measurements (GAIM) model, in particular the Gauss-Markov (GM) implementation [*Scherliess et al.*, 2004; *Schunk et al.*, 2004; *Thompson et al.*, 2006; *Scherliess et al.*, 2009]. AFRL has confirmed (albeit with some ongoing issues) [see, for example, *McNamara et al.*, 2010] that the GAIM-GM model is a very successful data assimilation model that provides generally reliable real-time specifications of the ionosphere. AFRL has now turned some attention to situations in which there is no data to assimilate, such as for the operationally important 4 day ionospheric forecasts.

[5] GAIM-GM is usually set up to make real-time specifications as well as ionospheric forecasts with a lead time up to ~6 h. After that, the utility of the latest assimilated data has decreased to a negligible level in line with the size of the autocorrelation coefficient. The autocorrelation coefficient for Australian values of foF2, for example, drops below 0.7 after only 1 or 2 h, depending on the level of solar activity, season and time of day (L. F. McNamara, Autocorrelation coefficients for deviations of foF2 recorded by ionosondes in the Australian region, unpublished report, 2009).

[1]Air Force Research Laboratory, AFRL/RVBX, Hanscom AFB, Massachusetts, USA.

[6] For the desired 4 day forecasts of the ionosphere in particular, one possible approach would be to run the Ionospheric Forecast Model (IFM) [*Schunk et al.*, 1997] or a similar model with 4 day forecasts of the disturbances to the Earth's magnetic indices (kp, Ap, for example). However, the IFM is very insensitive to even large changes to kp and Ap at low and midlatitudes and does not, in any way, match the observed storm time changes to the Australian ionosphere (McNamara, unpublished report, 2009).

[7] As a way forward, we have investigated the applicability of forecasting procedures used at different times in tropospheric weather forecasting, which are (1) numerical forecasting, (2) persistence forecasting, (3) trend forecasting, (4) climatological forecasting, and (5) analog forecasting. Numerical weather forecasting is based on the laws of physics and involves the assimilation of large numbers of observations and the solution of the coupled physical equations on very large computer systems. The GAIM-GM model uses similar data assimilation techniques. Numerical ionospheric forecasting could rely, for example, on the use of coupled thermospheric and ionospheric models, with drivers developed from separate solar activity, solar wind, MHD, and geomagnetic disturbance codes. Eventually, all of these codes would be integrated.

[8] A persistence forecast would assume that the ionosphere for the next 4 days will be the same as for the current day (like weather forecasts for a desert location). The forecast ionosphere would be four clones (for 4 days) of the GAIM-GM specification for the current day. These forecasts would be relatively good for quiet periods.

[9] In tropospheric trend forecasting, we look upstream (generally to the west) to see what the weather will be here tomorrow. In ionospheric trend forecasting, we would look to the Sun for trends in the fluxes and forecast the associated trend in the electron concentration of the ionosphere. Such trend forecasts would replace persistence forecasts if there is a trend in the solar flux. Once a solar event occurs or is forecast, we would have to adopt a more complicated approach (numerical, climatological, or analog).

[10] A climatological forecast could be based on past observations of storm effects on TEC (say), parameterized in some way to provide the typical ionospheric response to historical storms. This parameterization has been done for the United States [*Mendillo*, 2006], but apparently not globally. The U.S. studies cannot readily be applied to other longitude zones. The parameterization would be a large task, and we would end up with average storm morphologies.

[11] An analog forecast (arguing by analogy) would look to the past to locate a 4 day interval with basically the same geomagnetic indices as forecast by some space weather center (such as SWFL). For quiet conditions, we would take GAIM's current global specification and apply it to the next 4 days, as with persistence forecasts. If the 4 day forecasts of the geomagnetic field are for a "disturbed" interval, we would go back in time until we find a similar disturbed interval (same general level of solar activity, same season, etc.). By analogy, we would argue that the ionosphere for the next 4 days will be the same as it was for that historical disturbed interval (with possibly some adjustments for different general levels of the solar flux).

[12] We concentrate in this paper on the possibility of making useful analog ionospheric forecasts, as an interim measure until the numerical space weather codes have matured. The utility of analog forecasts is cast in the guise of the question: If I can specify a relevant global magnetic index correctly for the next 4 days, can I then obtain reliable 4 day analog forecasts of the global ionosphere?

[13] There are of course a few limitations and restrictions to this grand plan. To start with, we address only the midlatitude ionosphere, partly because the GAIM-GM model extends only to ±60° geographic latitude. We also limit our initial investigation to the Australian region, simply because manually scaled values of foF2 are then readily available for several solar cycles and multiple ionosonde locations. Australia itself is basically midlatitude, with the southern-most ionosonde being at Hobart (dip latitude of −57.9°). However, the northern-most ionosonde for which data are available is near the equator, at Vanimo (Papua New Guinea; dip latitude of −11.2°).

[14] Since we intend to compare the behavior of the ionosphere during different magnetically disturbed intervals, we need a suitable metric. We take as this metric the percentage change in the F2 region peak density (NmF2) from its median value at the same UT for a collection of magnetically quiet days in the same month. This type of metric is commonly used for investigating storm effects on TEC [*Mendillo*, 2006]. Since it is well known that ionospheric storms have seasonal variations, we split the storms up into (Southern Hemisphere) summer, equinoxes, and winter. Since it is also known that the storm time variation depends on the local time of the storm's start, we also split the storms up into those that started during the day and during the night.

[15] An analog forecast of the ionosphere at one of the Australian locations (Hobart, for example) would proceed as follows. (1) It is currently summer in Australia. (2) The global daily values of Ap for the next 4 days are forecast to be 15, 50, 75, and 24. (3) The storm will start at about 06UT (16LT) on day 2.

[16] So we go to a database of the ionospheric variations that occurred during historical disturbed intervals (1997 through 2006, in fact) and identify the one(s) that satisfy the three criteria: occurred during a summer month; Ap reached a peak between 60 and 100; the storm started during the day. With the "resolution" of the present sim-

plistic analog forecasting scheme, we find two storms. The forecast would then follow the commonality that can be gleaned from the two historical storms for Hobart that are illustrated later (storm 026 in Figure 6 and storm 147 in Figure 7). In fact, storms 026 and 147 are two of the only nine or so summer ionospheric storms that exhibit (subjectively) detailed similarities. As discussed in the paper, storms can be considered to be similar at various levels. If the objective is to track the detailed variation of a storm, including the short-lived positive phases that are often superimposed on a general negative phase, it is almost impossible to match individual storms. However, if it sufficient to match the evolution of only the main negative phase (the lower envelope of the variation) or to note that the storm time changes are multiple short-lived enhancements in NmF2 (low latitude, winter), more matches are possible, and the analog approach can provide valuable ionospheric information.

[17] Section 2 of this paper describes the sources of the ionospheric and geomagnetic data and the general methodology. Section 3 provides a brief summary of the expected storm time changes at the Australian ionosonde locations. These are already well known for "typical" storms. Section 4 presents the changes in NmF2 for Hobart, along with the variation of kp and Dst for six disturbed intervals (two per season). This is only a tiny subset of what would be possible (~190 storms, potentially 11 ionosondes). Section 5 illustrates some of the short timescale structures that exist in the positive phases of a storm (which an analog forecast would probably fail to reproduce) that are correlated for ionosondes from Hobart to Vanimo.

[18] The basis of analog forecasting is that the storms in a specific category should have similar storm time variations. Section 6 illustrates the consistency of the median variations for Hobart summer and equinoctial storms. Section 7 discusses the results of this pilot study and their implications for global analog ionospheric forecasts. Sections 8, 9, and 10 then discuss global analog ionospheric forecasts (the ultimate goal), physical modeling of the disturbed ionosphere, and the potential utility of analog forecasts.

[19] While this paper looks at the detailed evolution of ionospheric storms and finds that the storms are too individual for the analog approach to be "highly" useful, it is quite possible for an operational analog system to provide less detailed but still valuable ionospheric forecasts in the interim years preceding the deployment of successful numerical space weather codes.

[20] As mentioned at the start of this section, this is basically a concept paper. We present the analysis of Australian values of foF2 simply to illustrate the proposed methodology of analog forecasting. The ionospheric model of interest is the USU-GAIM model, as implemented now and (possibly) in the future by AFWA. Setting up the assimilation data for the GAIM model (as well as other storm time observations such as scintillation) for past and future disturbed intervals will be a large and complex task, which we expect to take us about 5 years, keeping pace with the increase in new disturbed intervals that will come with the next solar maximum. These new intervals are required in order to build up the statistics of disturbed intervals that will have enhanced GAIM assimilation data, such as slant TEC observations from an increasing number of ground sites, radio occultation TEC observations from new satellites, and profiles from an expanding number of ionosondes.

[21] There are other approaches to estimating the storm time development of the ionosphere, such as that developed by *Fuller-Rowell et al.* [2000]. This storm time correction model is designed to scale monthly medians of NmF2 and possibly TEC using an index derived from the previous 30 days of auroral or geomagnetic activity. It has been applied to the International Reference Ionosphere in the form of the IRI-STORM model, which has been evaluated, for example, by *Miró Amarante et al.* [2007]. We see no role for such an approach in our GAIM-centric analog forecasting scheme. Being an assimilative model, USU-GAIM will naturally reproduce (within reason) the observed assimilation data during a disturbed interval, in real time. This situation will improve as more assimilation data becomes available and as USU-GAIM is further developed.

[22] The other aspect of analog forecasting, which is the problem of forecasting the disturbed geomagnetic field, is a key task that is being addressed on a continuing basis by groups such as the AFRL Space Weather Forecasting Laboratory.

2. Sources of Data and General Methodology

[23] Eight Australian ionosondes have been considered, along with two (Vanimo and Port Moresby) in Papua New Guinea and one (Juliusruh/Rugen) in Germany. These are listed (alphabetically except for Juliusruh) in Table 1 and plotted in Figure 1 (excluding Juliusruh).

[24] The ionospheric data (manually scaled hourly values of foF2) was obtained from the IPS Radio and Space Services Web site (http://www.ips.gov.au/World_Data_Centre/1/3). The kp and Ap indices were obtained as "DGD.txt" files from the NOAA Web site (http://www.swpc.noaa.gov/ftpdir/indices/old_indices). Juliusruh/Rugen was included in the study because (1) its data has been added to the IPS database and is thus very readily accessible and (2) it is the Northern Hemisphere equivalent of Canberra, thus allowing simple summer/winter seasonal comparisons.

Table 1. Locations of Australian Ionosondes Plus Juliusruh, Germany

Latitude	Longitude	ID	DipLat	Station
−27.53	152.92	3859	−38.2	Brisbane
−35.52	149.0	3763	−48.6	Canberra
−12.45	130.95	3351	−23.2	Darwin
−42.92	147.32	3766	−57.9	Hobart
−22.25	114.08	2856	−36.6	Learmonth
−31.98	116.22	2961	−49.0	Mundaring
−29.03	167.97	4260	−37.0	Norfolk
−9.4	147.1	3750	−18.0	Port Moresby
−19.63	146.85	3755	−29.8	Townsville
−2.70	141.30	3546	−11.2	Vanimo
54.60	13.40	0318	+52.9	Juliusruh

[25] During a daytime negative phase of a storm, foF2 often decreases to a value less than foF1, in which case the data entry would read something like *E 45G*, with the qualifying letter E meaning less than and the descriptive letter G meaning that foF2 could be specified only as an upper limit because it had gone below foF1. Rather than ignoring substantial numbers of such records, we have simply taken the value 45 (4.5 MHz) as the actual value of foF2. This means that the percentage depressions of NmF2 that are plotted are sometimes underestimates. At other times during a storm, the common data entry is like *U 36F*, where the value 3.6 MHz is uncertain by less than 5% (U) because the F2 trace is spread (F). These U entries should not result in a bias in the storm time values of foF2.

[26] About 190 4 day disturbed intervals were identified manually for the period 1997 through 2006, using the DGD.txt data files. A disturbed interval was defined as one that starts with a quiet day (Ap < 25), followed by 1 or 2 days with Ap > 25. Most intervals had Ap < 25 for the fourth day. Some disturbed intervals were excluded because they ran into the following month, and most data processing was month-based. Some intervals that ran for longer than 4 days were excluded at a later step in the processing. (A point to consider when developing an operational system is that the ionosphere can sometimes be quite disturbed even if Ap < 25.)

[27] Sets of magnetically quiet days (usually Ap <10) were also identified manually for each month of the 10 years that contained a disturbed interval. The values of foF2 on these days were used to define the median quiet day variation of NmF2 for use with each disturbed interval.

[28] The computer program used for the current analysis will select those disturbed intervals that satisfy three requirements: the specified season, the specified start of the storm (day or night), and a magnetic index. Two magnetic indices have been considered, the global daily Ap value and the equatorial Dst index. The kp index is used only to define the starting time of the storm, which is taken as 1 h after the 3 h kp value first goes to 4. This is admittedly a relatively crude estimate, but it is sufficient for day/night decisions and perhaps typical of forecast accuracy. The storms have been divided into

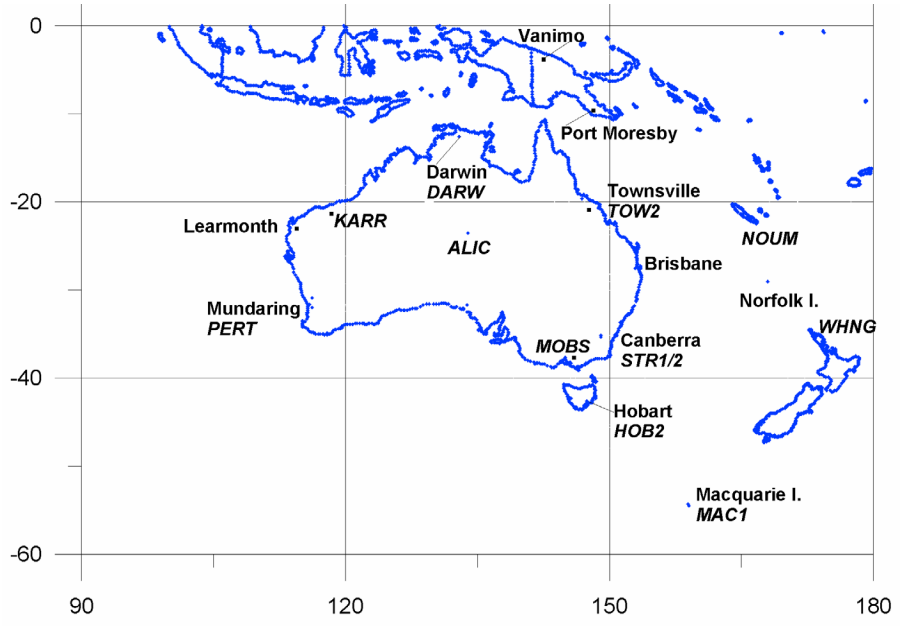

Figure 1. Ionosonde locations (mixed case) in Australia and Papua New Guinea. The all-caps locations are GPS TEC sites.

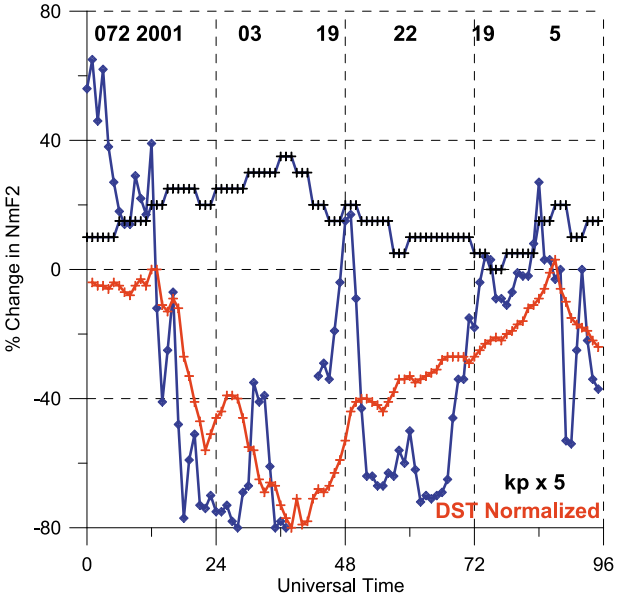

Figure 2. UT variation of the percentage changes in NmF2 for Hobart (blue diamonds), rescaled Dst (red crosses), and rescaled kp (black crosses) for 19–22 March 2001. Storm 072. Maximum Ap = 66. Minimum daily average Dst = −117.

different Ap bins (25–40, 40–60, 60–100, >100, >60) and (separately) into different daily average Dst bins (−10 to −50 nT; −50 to −100; −100 to −200; <−200). The results we present here are in terms of the Ap values, since it is expected that the 4 day geomagnetic forecasts made in the near future will be in terms of the Ap values. Using Dst would simply place the storms into different groups.

[29] Comparisons to date have been limited because the geomagnetic and ionospheric changes are presented graphically and compared manually. There would be potentially about 190 × 11 (disturbed intervals × number of ionosondes) storm responses to compare.

3. Expected Storm Time Behavior

[30] Ionospheric storms have positive phases (foF2 is increased above normal quiet day levels) and negative phases (foF2 is decreased). The main features of ionospheric storms are as follows [*Mendillo*, 2006; *Matsushita*, 1959]: (1) the positive phase lasts longer and becomes more prominent with decreasing latitude; (2) the positive phase is usually followed by a prolonged negative phase; (3) the negative phase gets stronger with increasing latitude; (4) when the positive phase has a noticeable local time component, its maximum amplitude occurs near 1800 LT at subauroral latitudes, earlier at higher latitudes and later at lower latitudes; and (5) positive storms are more pronounced in winter, and negative storms are more pronounced in summer.

[31] The negative phase of ionospheric storms results from enhanced chemical loss rates driven by changes in the thermosphere, while the positive phases are due to winds and/or electric fields. One of the latest reviews of ionospheric storms was written by *Buonsanto* [1999]. For a summary of the current state of affairs for TEC, see *Mendillo* [2006, section 9.1]. Some of the large increases in foF2 found in the present study are possibly associated with prompt penetration electric fields and the dayside ionospheric super fountain [*Tsurutani et al.*, 2008], although *Balan et al.* [2010] find that an equatorward neutral wind is required to produce positive ionospheric storms.

[32] The results presented here are mainly for Hobart, with one disturbed interval for each of Canberra, Brisbane, and Townsville (toward the equator). Negative storm effects (foF2 decreases) increase toward the pole, while positive effects (foF2 is enhanced) increase toward the equator.

4. Storm-Related Changes in NmF2 at Hobart

[33] The storm-related changes (especially the depressions of foF2) are largest at Hobart and for the largest geomagnetic storms. The changes plotted in Figures 2–10 are versus UT (for Hobart LT = UT + 10). Missing foF2 data leads to gaps in the NmF2 curve.

4.1. Equinoctial Storms

[34] Figure 2 shows the results for storm 072. The blue (diamonds) curve shows the percentage change in NmF2 (relative to the median quiet day values) versus universal time for Hobart, 19–22 March 2001 (storm 072). The maximum change in NmF2 is truncated to 80% in all plots. The red (+) curve shows the variation of the Dst index. The Dst values have been rescaled so that they reach a maximum negative value of −80 nT. The kp indices (staircase curve; black +) have been multiplied by five for presentation purposes. The storm started at ~13 UT on day 19 (defined as when the 3 hourly kp reaches 4, plus 1 h). The numbers at the top of Figures 2–10 are records from the master list of disturbed intervals: storm number, year, month, start day of disturbed interval, end day of disturbed interval, day of month in which kp passes through 3, and kp counter (1 through 8 for 3-hourly intervals).

[35] Figure 3 shows the results for the other disturbed interval (086) that satisfied the same three criteria (equinox, Ap between 60 and 100, and storm started at night). The highest value of Ap during the 4 day interval

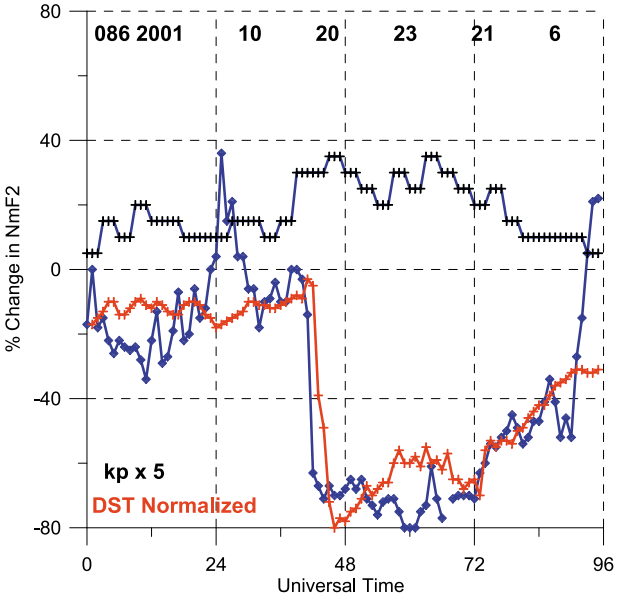

Figure 3. UT variation of the percentage changes in NmF2 for Hobart (blue diamonds), rescaled Dst (red crosses), and rescaled kp (black crosses) for 20–23 October 2001. Storm 086. Maximum Ap = 66. Minimum daily average Dst = −150.

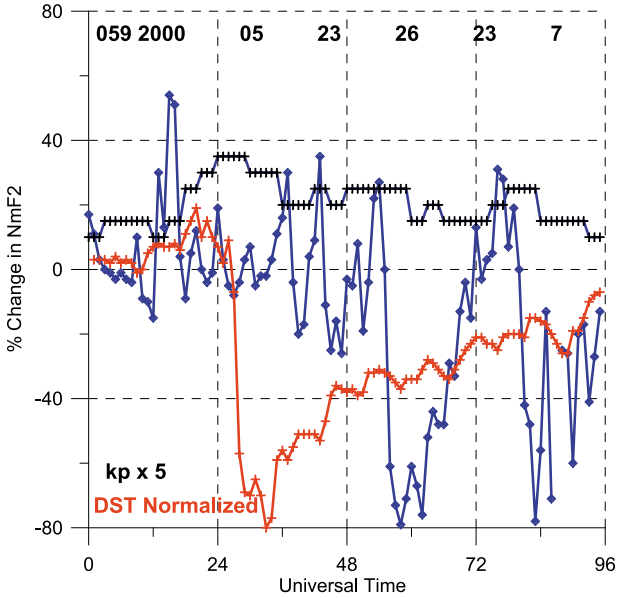

Figure 4. UT variation of the percentage changes in NmF2 for Hobart (blue diamonds), rescaled Dst (red crosses), and rescaled kp (black crosses) for 23–26 May 2000. Storm 059. Maximum Ap = 73. Minimum daily average Dst = −90.

was 66 for both storms, 072 and 086. There are both similarities and differences between the two NmF2 curves. Obviously the Dst curve provides a good reference for these storms. Both storms showed a decrease of ~80% in NmF2 following the onset of the Dst main phase, with a recovery back to prestorm levels after 2 or 3 days.

[36] The essential differences between the two ionospheric storms are (1) the rate at which NmF2 decreased (which was in line with the decrease in Dst) and (2) the two positive phases in NmF2 (back toward quiet time levels) for storm 072. Examination of similar plots for other storms suggests that positive phases in NmF2 will be superimposed on the onset of the main negative phase if the onset of the decrease in Dst is gradual (storm 072) rather than steep (storm 086).

4.2. Winter Storms

[37] Figures 4 and 5 show two of the three winter storms that started at night and had Ap values between 60 and 100. Winter storms are mostly characterized by enhancements in foF2, especially at low latitudes. The maximum Ap values were 73 for storm 059 and 86 for storm 133.

[38] There is no initial large depression of NmF2 for storm 059 (Figure 4), although there are erratic variations around the quiet day curve (which is the *x* axis). These

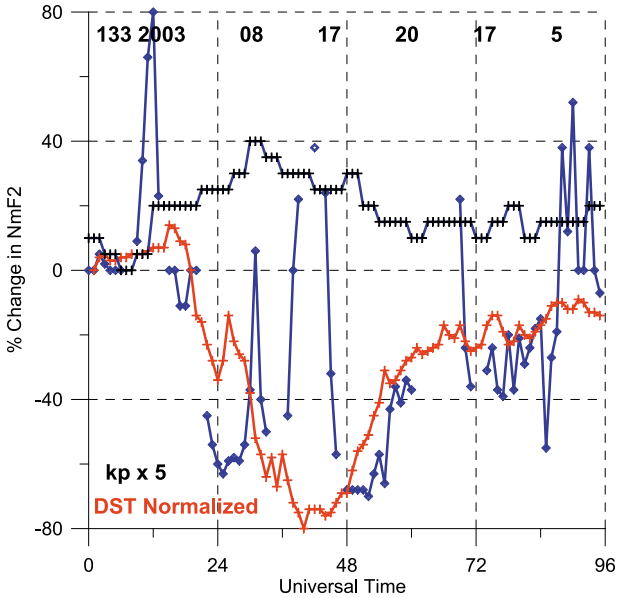

Figure 5. UT variation of the percentage changes in NmF2 for Hobart (blue diamonds), rescaled Dst (red crosses), and rescaled kp (black crosses), 17–20 August 2003. Storm 133. Maximum Ap = 86. Minimum daily average Dst = −108.

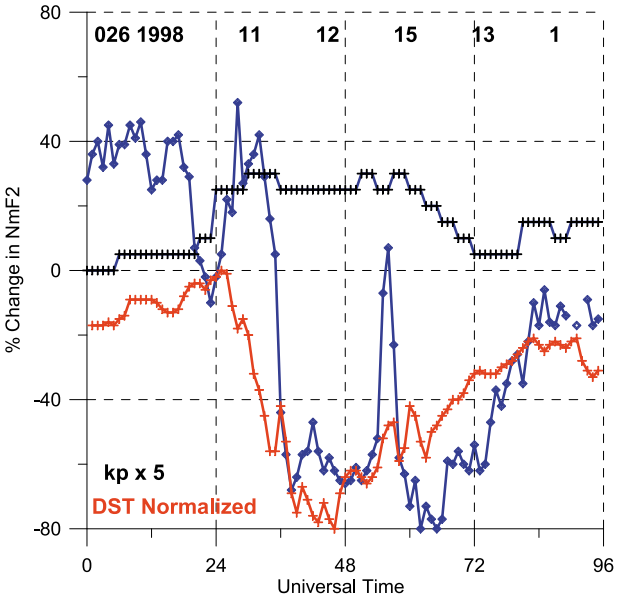

Figure 6. UT variation of the percentage changes in NmF2 for Hobart (blue diamonds), rescaled Dst (red crosses), and rescaled kp (black crosses), 12–15 November 1998. Storm 026. Maximum Ap = 60. Minimum daily average Dst = −83.

variations are probably associated with the substorm variations that can be seen in the Dst plot. In this case, unlike with Figure 3, even valid forecasts of Dst would not be useful. The steep decay of the Dst is once again not accompanied by any positive phases.

[39] Storm 133 (Figure 5), on the other hand, has a strong negative ionospheric phase, with decreases down to about −80%. The slope of the Dst onset is much less than for storm 059 (Figure 4), and this onset is marked by positive phases in NmF2.

[40] The two very different ionospheric responses for storms 059 and 133 show that the present three-class classification (season, day/night start, and Ap range) of disturbed intervals is sometimes not adequate to forecast the behavior of the ionosphere. (In fact, the ionospheric response to storm 059 is also quite unusual at Juliusruh. Canberra, Brisbane, Townsville and Vanimo showed mostly positive phases.)

4.3. Summer Storms

[41] Figures 6 and 7 show two of the three summer storms that started during the day and had Ap values between 60 and 100. The maximum Ap values were 60 for storm 026 and 62 for storm 147.

[42] The ionospheric responses shown in Figures 6 and 7 (as well as the third storm, 011) are very similar, with an initial positive phase in NmF2 as Dst falls, a delayed positive phase ~24 h later, and recovery to quiet day levels after 2 days. However, the decreases in NmF2 go down to about −70% for storms 011 and 026 and only to about −40% for storm 147.

4.4. Storm Selection Based on Dst

[43] In keeping with the daily nature of the Ap forecasts, the storms can optionally be grouped according to the daily average of the Dst index. However, grouping the storms in this way does not seem to offer any advantages over grouping them by Ap, and SWFL does not currently forecast values of Dst. The storms in each of the three pairs presented above all had similar daily Dst values.

5. Consistent Storm Effects at Different Latitudes

[44] Winter storms at the lower latitude sites (approximately Brisbane and equatorward) usually result in positive phases rather than negative phases. The positive phases are not single features but rather are made up of multiple short-term oscillations in NmF2. The figures presented in this section (Figures 8–10) are for a winter storm, 059, which occurred during 23–26 May 2000. The

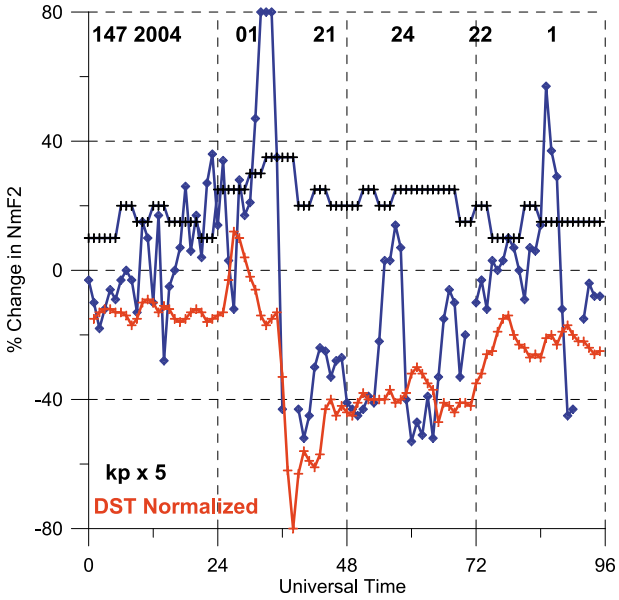

Figure 7. UT variation of the percentage changes in NmF2 for Hobart (blue diamonds), rescaled Dst (red crosses), and rescaled kp (black crosses) for 21–24 January 2004. Storm 147. Maximum Ap = 62. Minimum daily average Dst = −73.

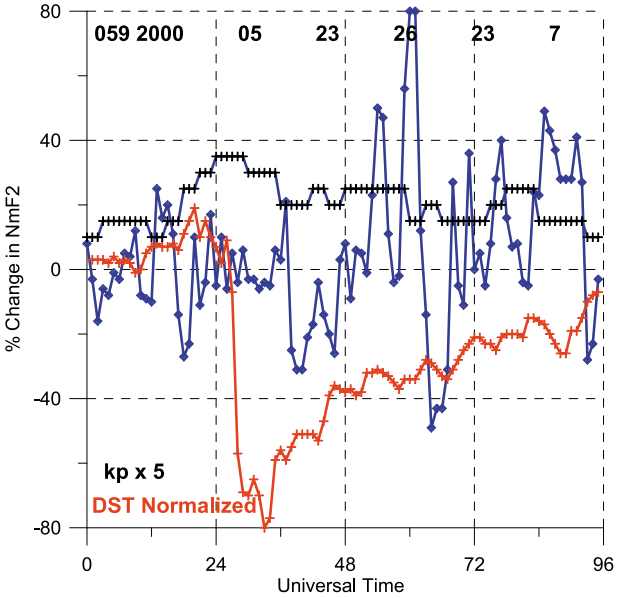

Figure 8. UT variation of the percentage changes in NmF2 for Canberra (blue diamonds), rescaled Dst (red crosses), and rescaled kp (black crosses) for 23–26 May 2000. Storm 059.

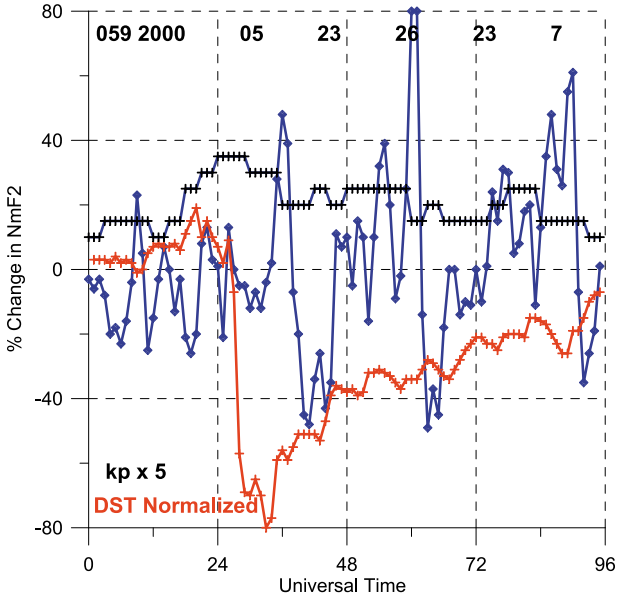

Figure 9. UT variation of the percentage changes in NmF2 for Brisbane (blue diamonds) and rescaled Dst (red crosses) for 23–26 May 2000. Storm 059.

largest value of Ap was 73, and the smallest daily average value of Dst was −90 nT. Figures 8, 9, and 10 show the variations for Canberra, Brisbane, and Townsville. The Hobart plot for this storm was presented earlier as Figure 4.

[45] Hobart (Figure 4) is the only location that shows a consistent negative phase. This is as expected. Note that there is no obvious relation between the Dst and changes in NmF2 for this winter storm. Even a successfully forecast Dst index would be a poor indicator of the ionospheric response to a winter storm.

[46] The minimum in the value of NmF2 for Hobart that occurs at hours 57–59 (09–11 on day 25) also appears ~3 h later in the Canberra, Brisbane, and Townsville plots, but with lower amplitude. The change in NmF2 at Hobart is ~80%, whereas it is only ~40% at the other three sites. There is also a matching decrease in NmF2 near hour 84 (12 UT on day 26). The decrease near hour 60 can also be seen at Vanimo, which showed a depression of ~80% at hours 62 and 63.

[47] The oscillating positive phases seen in Figures 9 and 10 are possibly due to electric fields, which in their turn are related to the substorms that can be seen as oscillations in the Dst index. The positive phases are also consistent for the four locations for storm 021 (5–8 August 1998).

[48] From the point of view of analog forecasts, it seems highly unlikely that two (winter) storms will have

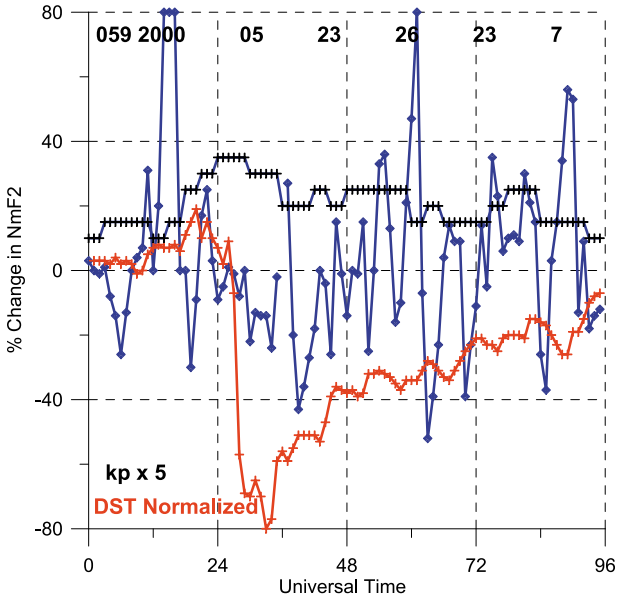

Figure 10. UT variation of the percentage changes in NmF2 for Townsville (blue diamonds) and rescaled Dst (red crosses) for 23–26 May 2000. Storm 059.

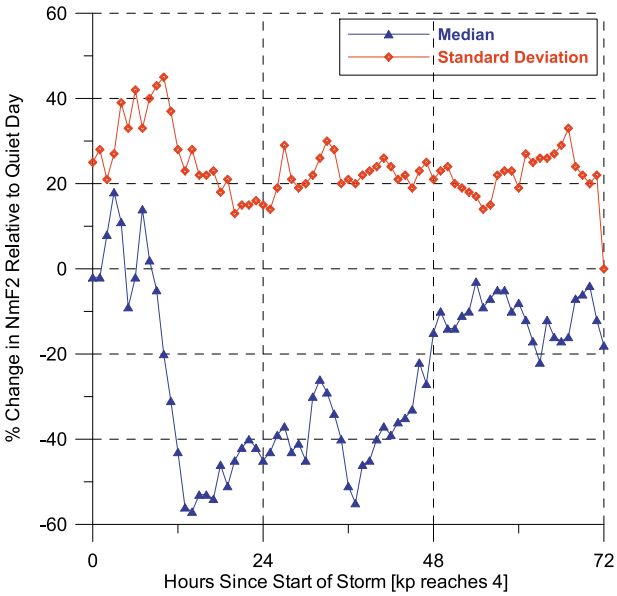

Figure 11. Storm time variation of the percentage changes in NmF2 for Hobart, all summer storms with Ap > 25, daytime starts. $N = 15$. Median, blue triangles; standard deviation, red diamonds.

the same substorm activity and oscillatory positive phases in NmF2. Thus, they will not be "similar" in detail. However, they will be similar in having oscillatory positive phases and probably no negative phase at lower latitudes.

6. Median Storm Effects

[49] The basis of analog forecasting is that the storms in a specific category should have similar storm time variations. We saw in the previous section that the positive phases that are the feature of winter storms are very structured and that this structure would not be expected to be the same for different storms. Consistent storm time variations can be seen, however, in the summer and equinoctial storms, especially for Hobart since it has the largest negative phases.

[50] Figures 11 and 12 show the median and standard deviation of the percentage changes in NmF2 at Hobart for summer and equinoctial storms, respectively. The time scale is storm time, i.e., hours after the 3 hourly kp reached a value of four (plus 1 h).

[51] Figures 11 and 12 are for storms that started during the day. Both Figures 11 and 12 show a positive phase at the start of the storm, but the standard deviations are very high. They also show a delayed positive phase at ~30 h, but the standard deviations are again very high (because the positive phases vary in strength and duration).

[52] The negative phase between about hours 12–24 is deeper than the value of the standard deviation, especially for summer (Figure 11). The same situation holds for the decrease after the delayed positive phase. The median curves can thus be considered to be realistic during these times. The large storms (Ap > 60; not shown) show consistent behavior in all three seasons, but the sample sizes for each season and day/night start time are small (~6).

7. Discussion

[53] As a basis for investigating the utility of analog forecasts, we have chosen to use manually scaled values of foF2 at Australian ionosonde stations run by IPS Radio and Space Services. These values of foF2 are very easy to obtain and go back to 1957 at the key stations. There is thus ample data to define storm time variations for hundreds of storms and at multiple locations. The logic is that if analog forecasts based on this easily accessible ionospheric data are shown to offer some value for these low and midlatitudes sites, a much larger effort could be expended in more difficult investigations.

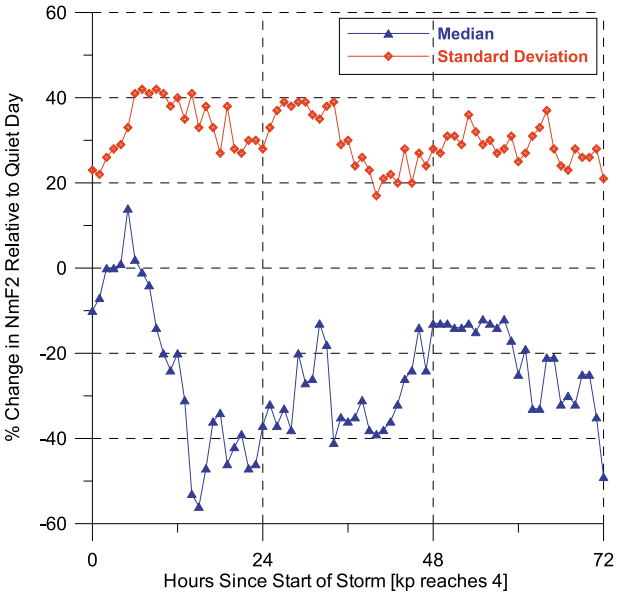

Figure 12. Storm time variation of the percentage changes in NmF2 for Hobart, all equinox storms with Ap > 25, daytime starts. $N = 21$. Median, blue triangles; standard deviation, red diamonds.

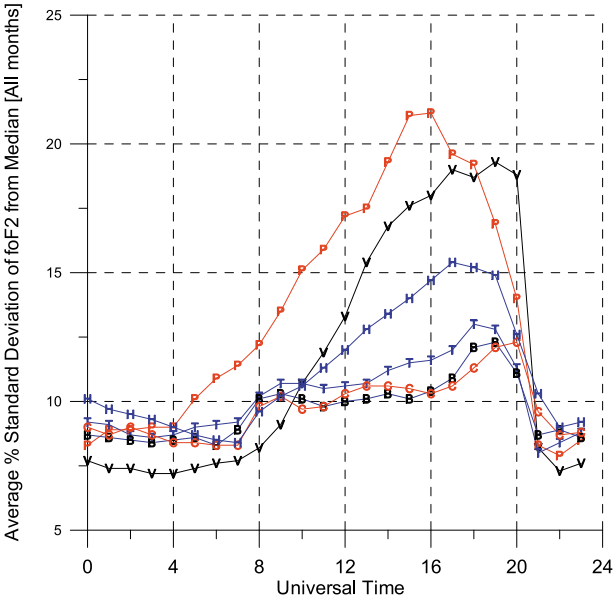

Figure 13. Diurnal variation (versus UT) of the standard deviation of the percentage differences of foF2 from the median value for quiet days, averaged over all months containing a disturbed interval. V, Vanimo; P, Port Moresby; T Townsville; B, Brisbane; C, Canberra; H, Hobart.

[54] We have chosen to work in terms of the daily Ap because that is the geomagnetic index most likely to be provided as a forecast in the early interim years preceding the deployment of numerical space weather codes. Choosing the maximum value of Ap in a 4 day interval is consistent with the likely uncertainties in the forecast values of Ap.

[55] Two ionospheric storms can be different in several ways that make it unlikely that any two storms can be described as having similar variations, even if they are characterized by the same Ap index: (1) the rate at which NmF2 falls at the start of a (negative) storm, (2) the largest depression in NmF2, (3) the duration of the depression in NmF2, (4) the amplitude and duration of initial and delayed increases in NmF2, and (5) the presence (amplitude, periodicity) of short-lived enhancements in NmF2.

[56] Some storms, such as storm 086 (Figure 3), start precipitously, tracking the decrease in Dst. This storm started at night (at Hobart). In contrast, storm 072 (Figure 2) starts more slowly (again at night), decreasing to its maximum depression over a period of ~12 h.

[57] The percentage changes in NmF2 at Hobart usually reach about −80% for the larger storms. This near-constancy is a measure of the utility of the percentage change as a storm time metric. The depression in NmF2 usually lasts 1 day and possibly 2 days. The ionosphere will start to be replenished at sunrise on the last day of the disturbed interval.

[58] The enhancements in foF2 can be long-lived, as with the daytime onset of storms 026 (Figure 6) and 147 (Figure 7). Other enhancements last only 1 or 2 h, as during the recovery phase for storms 026 and 147. Some of these shorter-lived enhancements appear to be related to substorm structure in the Dst variation.

[59] The basic problem that we have encountered here is that the selection procedure based on the three simple criteria (season, day/night start of storm, and range of Ap) produces multiple disturbed intervals that can have quite dissimilar variations of NmF2. Subjective examination of figures such as Figure 7 for many more storms and for other ionosonde locations (laid out in arrays of thumbnail plots) has identified only nine storms that had variations that were consistent in some detail with those in the same group. These were all equinoctial storms.

[60] The Dst index curves have been scaled to a maximum depression of 80 nT in Figures 2–10. Thus, the NmF2 for Hobart and the Dst variations tend to track each other for some summer and equinoctial storms, suggesting that all problems would be resolved if reliable 4 day forecasts of Dst were available. However, for other storms (especially winter storms), the Dst and NmF2 variations are completely different, with the ionosphere exhibiting mainly positive phases, regardless of the variations of Dst.

[61] It is interesting to note that the empirical ionospheric storm time correction model developed by *Fuller-Rowell et al.* [2000] is also less successful for winter storms. For use of this model in a forecast mode, 4 day forecasts of the auroral power index [*Evans et al.*, 1988] would be required.

[62] It is well known that there is a significant day-to-day variability of foF2 about the monthly median (the ionospheric weather). For example, *Wilkinson* [2004] gives the canonical values of 0.85 and 1.15 for the lower and upper deciles of the distribution. That is, 80% of all observations (without regard to magnetic activity) lie within ±15% of the median. We are interested here in the variability that occurs for magnetically quiet days, because it sets a minimum uncertainty on analog forecasts of foF2/NmF2 for such conditions. As described in section 2, the quiet day reference curves for each disturbed interval were defined as the median for days in that same month with Ap less than or equal to 10. The standard deviation of the quiet day values of foF2 about that median has also been calculated for each month containing a disturbed interval. Figure 13 shows the diurnal variation (versus UT) of the average over all quiet

days of the standard deviation of the percentage difference of the observed values of foF2 from the median.

[63] There is a curve for each of the six ionosondes near 150°E (Vanimo, Port Moresby, Townsville, Brisbane, Canberra, and Hobart). For the "safely midlatitude station," Townsville, Brisbane, and Canberra, the standard deviation is ~10%. It is lower during the day (21–07 UT; 07–17 LT) than at night, when the values of foF2 are lower. The highest values of the standard deviation occur for Port Moresby (P) and Vanimo (V) at night, with Hobart (H) in between. The standard deviations are generally higher at solar minimum than at solar maximum and higher in winter and the equinoxes than in summer. The standard deviations for NmF2 would be twice the foF2 values.

8. Global Analog Ionospheric Forecasts

[64] Most of the previous discussion was related to the observed values of foF2 for Australian ionosonde sites. For this special situation, with decades of reliable values of foF2, the forecast values of foF2 for disturbed intervals could also be based on the observed median storm time variations of NmF2 (such as Figure 11), as well as on analog forecasts. However, things are much more complex for global forecasts of the complete plasma frequency profile.

[65] We first considered analog forecasts in terms of a global ionospheric model, in particular the Utah State University GAIM-GM model, with a view to providing 4 day ionospheric forecasts based on forecasts of geomagnetic indices such as Ap. Being an assimilative model, GAIM-GM is able to track ionospheric changes due to storms, although it tends to be a little conservative with regard to the full extent of the storm values of the assimilated data [*Decker and McNamara*, 2007]. The proposed methodology is discussed here because of the operational importance of global forecasts for planning and mitigation purposes. Even uncertain forecasts should provide the essential variations of a forecast ionospheric storm, and be of some operational use.

[66] The basic idea would be to build up a database of GPS TEC (and other observations that are assimilated by GAIM) for historical disturbed intervals. An analog GAIM forecast specification would be obtained for a 4 day forecast interval by running GAIM with the assimilation data for a matching historical disturbed interval. The global modeling capability of GAIM is an essential part of the methodology, since it fills in the gaps between sites in a physically consistent fashion. Adjustments of the TEC observations could be made for different general levels of the solar flux, by using the observed linear dependence of TEC on an ionospheric index [*McNamara and Smith*, 1982]. Such a step should probably be avoided and can in fact be avoided if there are sufficient historical disturbed intervals.

[67] Using a database of assimilation data rather than a database of GAIM specifications would permit the use of the latest version of the GAIM model, such as the GAIM-FP (full physics) model [*Scherliess et al.*, 2009]. Quality control algorithms can also be applied to the historical data. This is difficult to do in real time, especially for TEC observations. As a proxy for ground truth observations, we would take the post facto GAIM specifications for the forecast interval, with GAIM assimilating the available (but withheld for the forecasts) data. Non-GAIM-related historical observations such as VHF and GHz scintillation could be added to the analog forecasts. Given a choice, the latest suitable reference interval would be preferred because there is probably more assimilation and other relevant data available.

[68] One of the difficulties with the analog approach is that the data assimilated by GAIM-GM is currently available for only about half a solar cycle, so the number of reference disturbed intervals is limited. However, the next solar cycle will hopefully provide substantially more reference intervals, with increased amounts of assimilation data (such as GPS TEC from more sites and probably radio occultation observations of TEC).

9. Physical Modeling of the Disturbed Ionosphere

[69] We have concluded that two storms with the same three criteria (for example, equinox, Ap between 60 and 100, and storm started at night) are rarely similar in the demanding sense that the storms should have matching short-lived positive phases and have the same percentage depression in NmF2. Storms with the same value of Ap can in fact have quite different detailed storm time variations.

[70] It therefore follows that a physical model of the ionosphere driven with these same criteria (forecast values of daily Ap, in particular) cannot reproduce the observed variations in NmF2 for a particular storm. All it can hope to do is to provide an average variation of some sort. An analog forecast would, on the other hand, contain realistic variations of the disturbed ionosphere with which operational systems would be required to cope, such as the short-lived doubling of NmF2 and TEC (by inference) during positive phases.

10. The Expected Utility of Analog Forecasts

[71] Visual comparison of the storms in the same category for Australian values of NmF2 has shown that the detailed storm behavior is not closely defined by Ap.

Two storms with the same Ap can have very different detailed behavior, such as the oscillatory positive phases for winter storms that were illustrated in section 5. Analog ionospheric forecasts will thus have limited validity.

[72] However, analog forecasts offer significant improvements over the current physical models of the ionosphere, which are insensitive at low and midlatitudes to geomagnetic disturbances because their component models are based on average conditions. Even if the analog forecasts get the details wrong, there is a high probability that they will represent the essence of the storm time behavior and provide useful information to operational systems.

[73] The concept of "global" (in the USU-GAIM sense of ±60° latitude) analog ionospheric forecasts is still in its infancy, and it could be 5–10 years before such forecasts are practicable, if only because analog forecasts rely on a large database of previous cases. While that database is being established, improved methodologies could be developed, such as one for better geomagnetic characterization and forecasting of disturbed intervals.

[74] The division of storms into those due to coronal mass ejections and to high speed solar wind streams from coronal holes would appear to offer some increase in utility of analog forecasts. Consideration should also be given to using Dst in place of Ap, if reliable forecasts of Dst become available. The geomagnetic index used as the key for searching past records can be changed easily as experience dictates. For example, *Fuller-Rowell et al.* [2000] and *Araujo-Pradere et al.* [2006] use an integral over the last 33 h of the 3 hourly Ap index.

[75] When fully developed, an analog ionospheric forecasting scheme could set the standard of what is possible. The numerical Space Weather models will have reached a significant milestone when they can provide more reliable ionospheric forecasts than the analog approach.

[76] **Acknowledgments.** The values of foF2 were downloaded from the IPS Radio and Space Services Web site (http://www.ips.gov.au/World_Data_Centre/1/3), the Dst indices from the Kyoto University Web site (http://wdc.kugi.kyoto-u.ac.jp/dstdir/index.html), and the kp and Ap indices from the NOAA Web site (http://www.swpc.noaa.gov/ftpdir/indices/old_indices).

References

Araujo-Pradere, E. A., T. J. Fuller-Rowell, and P. S. J. Spencer (2006), Consistent features of TEC changes during ionospheric storms, *J. Atmos. Sol. Terr. Phys.*, *68*, 1834–1842, doi:10.1016/j.jastp.2006.06.004.

Balan, N., K. Shiokawa, Y. Otsuka, T. Kikuchi, D. Vijaya Lekshmi, S. Kawamura, M. Yamamoto, and G. J. Bailey (2010), A physical mechanism of positive ionospheric storms at low latitudes and midlatitudes, *J. Geophys. Res.*, *115*, A02304, doi:10.1029/2009JA014515.

Buonsanto, M. J. (1999), Ionospheric storm—A review, *Space Sci. Rev.*, *88*, 563–601, doi:10.1023/A:1005107532631.

Decker, D. T., and L. F. McNamara (2007), Validation of ionospheric weather predicted by Global Assimilation of Ionospheric Measurements (GAIM) models, *Radio Sci.*, *42*, RS4017, doi:10.1029/2007RS003632.

Evans, D. S., T. J. Fuller-Rowell, S. Maeda, and J. Foster (1988), Specification of the heat input to the thermosphere from magnetospheric processes using TIROS/NOAA auroral particle observations, in *Astrodynamics 1987: Proceedings of the AAS/AIAA Astrodynamics Conference Held August 10–13, 1987, Kalispell, Montana*, *Adv. Astronaut. Sci. Ser.*, vol. 65, edited by J. K. Soldner et al., pp. 1649–1667, Univelt, San Diego, Calif.

Fuller-Rowell, T. J., E. Araujo-Pradere, and M. V. Codrescu (2000), An empirical ionospheric storm time correction model, *Adv. Space Res.*, *25*(1), 139–146, doi:10.1016/S0273-1177(99)00911-4.

Matsushita, S. (1959), A study of the morphology of ionospheric storms, *J. Geophys. Res.*, *64*(3), 305–321, doi:10.1029/JZ064i003p00305.

McNamara, L. F., and D. H. Smith (1982), Total electron content of the ionosphere at 31°S, 1967–1974, *J. Atmos. Terr. Phys.*, *44*(3), 227–239., doi:10.1016/0021-9169(82)90028-9.

McNamara, L. F., J. M. Retterer, C. R. Baker, G. J. Bishop, D. L. Cooke, C. J. Roth, and J. A. Welsh (2010), Longitudinal structure in the CHAMP electron densities and their implications for global ionospheric modeling, *Radio Sci.*, *45*, RS2001, doi:10.1029/2009RS004251.

Mendillo, M. (2006), Storms in the ionosphere: Patterns and processes for total electron content, *Rev. Geophys.*, *44*, RG4001, doi:10.1029/2005RG000193.

Miró Amarante, G., M. C. Santamari, K. Alazo, and S. M. Radicella (2007), Validation of the STORM model used in IRI with ionosonde data, *Adv. Space Res.*, *39*, 681–686, doi:10.1016/j.asr.2007.01.072.

Scherliess, L., R. W. Schunk, J. J. Sojka, and D. C. Thompson (2004), Development of a physics-based reduced state Kalman filter for the ionosphere, *Radio Sci.*, *39*, RS1S04, doi:10.1029/2002RS002797.

Scherliess, L., D. C. Thompson, and R. W. Schunk (2009), Ionospheric dynamics and drivers obtained from a physics-based data assimilation model, *Radio Sci.*, *44*, RS0A32, doi:10.1029/2008RS004068.

Schunk, R. W., J. J. Sojka, and J. V. Eccles (1997), Expanded capabilities for the ionospheric forecast model, *Rep. AFRL-VS-HA-TR-98-0001*, pp. 142, Air Force Res. Lab., Hanscom Air Force Base, Mass.

Schunk, R. W., et al. (2004), Global Assimilation of Ionospheric Measurements (GAIM), *Radio Sci.*, *39*, RS1S02, doi:10.1029/2002RS002794.

Thompson, D. C., L. Scherliess, J. J. Sojka, and R. W. Schunk (2006), The Utah State University Gauss-Markov Kalman filter of the ionosphere: The effect of slant TEC and electron

density profile data on model fidelity, *J. Atmos. Sol. Terr. Phys.*, *68*(9), 947–958, doi:10.1016/j.jastp.2005.10.011.

Tsurutani, B. T., et al. (2008), Prompt penetration electric fields (PPEFs) and their ionospheric effects during the great magnetic storm of 30–31 October 2003, *J. Geophys. Res.*, *113*, A05311, doi:10.1029/2007JA012879.

Wilkinson, P. J. (2004), Ionospheric variability and the international reference ionosphere, *Adv. Space Res.*, *34*, 1853–1859, doi:10.1016/j.asr.2004.08.007.

G. J. Bishop, L. F. McNamara, and J. A. Welsh, Air Force Research Laboratory, AFRL/RVBX, 29 Randolph Rd., Hanscom AFB, MA 01731, USA. (leo.mcnamara@kirtland.af.mil)